IJME

Int. J. of Applied Mechanics and Engineering, 2026, vol.???, No.???, pp.???-???
DOI: 10.59441/ijame/220079

SHAPE OPTIMIZATION OF COMPRESSED RODS CONSIDERING MATERIAL AND GEOMETRIC UNCERTAINTY: AN ANALYTICAL – STOCHASTIC APPROACH

M. Sadowski
Independent Researcher, POLAND
E-mail: miroslaw.sadowski@gmail.com

The article presents a stochastic approach to the shape optimization of compressed rods, taking into account random deviations of Young's modulus and the second moment of area. The parameters are described as stationary random fields with a specified correlation length, and their influence on the critical buckling load is determined using a first-order perturbation expansion. The obtained expressions for the expected value and variance of the critical load made it possible to assess the sensitivity of the structure to local stiffness disturbances. Subsequently, a probabilistic optimization problem was formulated within a family of Gaussian-type profiles, with the aim of minimizing mass while maintaining the required level of reliability. Numerical analysis shows that accounting for uncertainties makes it possible to obtain a rod approximately *12 %* lighter than the reference rod, without reducing load-carrying capacity. The presented approach demonstrates that modeling.

Key words: stochastic analysis, Rayleigh quotient, material and geometric uncertainty, shape optimization, Gaussian profile, reliability index, Wolfram Mathematica, buckling.

1. Introduction

Since antiquity, engineers and designers have sought optimal shapes of compressed rods that make it possible to reduce the mass of the element while maintaining its load-bearing capacity, or conversely – to increase the load-bearing capacity with constant mass. This phenomenon can already be observed in the *entasis* of Doric columns, and today also in aerospace and automotive structures, where elements must combine high load capacity with minimal mass. Such a formulation of the problem leads directly to the issue of structural stability optimization, that is, the search for an optimal solution that meets the specified design criteria. The critical buckling load plays a key role here, and its optimization is the main objective of the design process. Verification of the obtained solutions is carried out through analysis of the appropriate differential stability equation.

The scientific investigation of shape optimization for compressed rods began in the 18th century, namely Lagrange [1] formulated the problem of maximizing the buckling load for a prismatic rod of given length and volume – today known as Lagrange's problem. This is a classic example of optimization of slender structures with a mass constraint. In the 19th century, an important contribution to the development of this field was made by Clausen [2], who was one of the first to propose specific geometric profiles leading to an increase in buckling capacity. In subsequent years, the topic was continued by, among others, Blasius [3] and Ratzerdorfer [4], who investigated the influence of variable support conditions and multiple types of loading on the optimal shape of rods. Also noteworthy is the work of Jasiński [5], published in the French journal *Annales des Ponts et Chaussées*, in which the author analyzed the influence of geometric imperfections on the load-bearing capacity of rods – an issue still relevant in the design of modern thin-walled structures.

From the second half of the 20th century onward, significant advances were made in mathematical and numerical optimization methods. Keller *et al.* [6] used variational calculus to determine optimal distributions of bending stiffness. Gajewski [7, 8] dealt with shaping rods made of nonlinear elastic materials and analyzed their behavior under nonconservative loads. During this period, Filipow *et al.* [9] applied Pontryagin's maximum principle to the modeling of rods compressed by concentrated and continuously distributed forces,

obtaining exact solutions for various load cases. Atanacković *et al.* [10] applied Pontryagin's maximum principle to the optimization of a Pflüger rod, extending the classical approach to include generalized boundary conditions and more complex loading schemes.

In recent decades, there has been a growing interest in semi-analytical and numerical methods that take into account more realistic working conditions of structures. Erdönmez *et al.* [11] used the differential transform method (DTM) to analyze rods with variable cross-sections subjected to various types of loads – including eccentric and follower loads – demonstrating a significant possibility of mass reduction while maintaining the required load capacity. Parastesh *et al.* [12] presented a method for shape optimization of cold-formed steel beam-rods using a genetic algorithm, taking into account technological constraints, varied eccentricities and element lengths, and load capacity analysis using the DSM method, showing that more complex cross-sections are not always advantageous, and that optimal shapes reach *110 – 222 %* of the capacity of the reference section. New analytical approaches were also proposed by Marcinowski *et al.* [13], who applied the complex error function (ERFI) to describe the shape of a compressed rod, enabling a closed-form analytical solution of the buckling equation with parameterized curvature. In a subsequent paper [14], these authors developed an effective design procedure for steel tubular rods with variable cross-sections and variable wall thickness: the obtained results indicate a possible increase in load capacity from *60 %* up to even *170 %* compared with cylindrical reference rods of the same mass and length. Botis *et al.* [15] present a finite element model for analyzing rods with stepped and continuous cross-section variation, showing that appropriate shaping of the moment of inertia – particularly with a trapezoidal profile – can increase buckling capacity by as much as a factor of *3.556*, and selected configurations with stepped variation achieve values comparable to rods with a sinusoidal stiffness distribution. Xu *et al.* [16] analyze topology optimization of structures with consideration of buckling and propose a new algorithm maximizing the buckling load factor (BLF), based on a linear material interpolation model, which simplifies the optimization process, eliminates penalization problems, and ensures clearly better results than previously used methods. Uysal [17] demonstrates that cryogenic modification of CFRP increases the buckling capacity of adhesively bonded beams – in systems with steel and aluminum by *5.6 %* and *3.7 %*, respectively – confirming the positive influence of cryogenic treatment on the stability of the element. Meanwhile, Dahlberg *et al.* [18] applied the reduced-order modeling (ROM) method to fast shape optimization with a buckling constraint. The obtained approach made it possible to significantly shorten computation time while maintaining accuracy, which is particularly important in complex structures with many degrees of freedom. In further work, Ruocco *et al.* [19] presented an interesting approach to optimizing the buckling resistance of beams with variable cross-sections, combining an improved Hencky-type model with neural networks and a genetic algorithm, which enables fast and precise prediction of critical loads and significantly reduces computational cost compared with classical methods. Ferrari *et al.* [20] proposed a breakthrough optimization approach that also takes into account the initial post-buckling behavior of the structure. By introducing asymptotic expansion coefficients of the equilibrium path (in the sense of Koiter – Budiansky) into the objective function, they enabled the design of structures less sensitive to imperfections and more reliable under conditions exceeding the critical load.

Despite significant achievements, many of the existing approaches remain strictly deterministic. This applies both to solutions based on a prescribed family of functions describing the distribution of the moment of inertia, whose purpose is to maintain buckling capacity while reducing mass, and to increasing capacity with a fixed mass. Meanwhile, contemporary research is moving toward integrating analytical and probabilistic tools that allow for the inclusion of inevitable technological, material, and operational deviations (Morse *et al.* [21]; Ferreira Filho *et al.* [22]). Most of these studies, however, are based on numerical or heuristic approaches, such as genetic algorithms or evolutionary methods.

The above indicates that, in practical design, it must be kept in mind that the material and geometric parameters of rods are not strictly constant quantities. They may exhibit variability due to dimensional tolerances, material nonuniformity (fibers, porosity, residual stresses), and changing environmental conditions. As a result, both the moment of inertia and Young's modulus must be treated as random quantities, which leads to variable bending stiffness of the rod along its length. Importantly, such variability does not have to be treated solely as a negative factor. On the contrary, it may be used constructively. Proper consideration of random geometric and material deviations makes it possible to further reduce the mass of a rod determined in

a deterministic formulation while maintaining the required buckling capacity. The present article is an attempt to carry out such a process; this is its primary objective.

Below, the deterministic formulation of the problem is first presented, followed by its stochastic form with perturbation expansion, which makes it possible to evaluate the expected value and variance of the critical load and to formulate an optimization problem with a reliability constraint

2. Scope of the study

In the considerations, a compressed rod pinned at both ends, whose bending stiffness varies along its length, is analyzed (Fig.1).

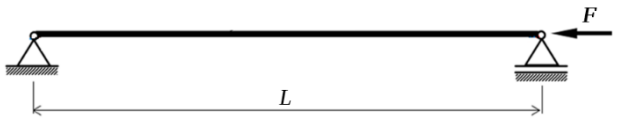

Fig.1. Static scheme of the system.

For comparison purposes, a reference rod with a constant circular cross-section and the same length is also adopted (Fig.2). The cylindrical rod serves as a reference point for the subsequent stages: determining the deterministic profile with the same critical load and lower mass, and later the optimal profile in the probabilistic sense.

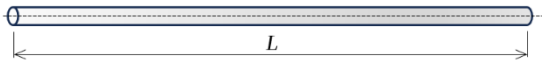

Fig.2. Reference cylindrical rod.

In the further analysis, it is assumed that the buckling mode can be approximated by a function satisfying the boundary conditions $\left[w(x)\right]_0^L = \left[w''(x)\right]_0^L = 0$, that is

$$w(x) = A\sin \pi x / L, \tag{2.1}$$

where A denotes the buckling amplitude. This choice is motivated by the fact that the curvature of the buckling function attains its maximum in the central part of the rod, which implies that bending strains and local elastic energy are concentrated in this region. This feature is of particular importance when analyzing the influence of random fluctuations of the second moment of area on the load-carrying capacity of the structure, since disturbances in the region of greatest curvature have the strongest effect on the critical buckling load. It should be emphasized that the assumed buckling function (2.1) represents an admissible approximation rather than an exact solution for the optimized rod; possible sensitivity of the quantitative results to alternative admissible functions satisfying the same boundary conditions is not addressed in the present study. It is further assumed that the function $I(x)$ describes the distribution of the second moment of area along the length of the rod according to the relation

$$I(x) = I_0 \exp\left(a(x - L/2)^2\right), \tag{2.2}$$

where I_0 is the value of the second moment of area at the mid-length of the rod, while a denotes the shape parameter of the profile (Fig.3). The adopted Gaussian-type family of profiles provides a compact parametric description of the second moment of area and enables an analytical formulation of the optimization problem.

Consequently, the obtained solution should be interpreted as optimal within the adopted family of admissible profiles, while alternative functional families may potentially yield different or improved mass reductions.

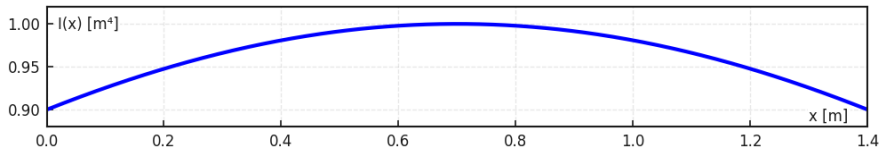

Fig.3. Example distribution of the second moment of area $I(x)$ along the length of the rod $(a=-0.215,\ L=1.4\,m)$.

The material parameters of the rod are fully described by Young's modulus E. The deterministic profile determined in this way minimizes the mass while preserving the critical load of the reference rod. In practice, however, the material and geometric parameters exhibit scatter – which motivates the transition to a stochastic formulation.

3. Stochastic model of the system

In the further part of the study, a stochastic model is formulated that makes it possible to quantitatively represent the influence of random material and geometric deviations on the behavior of the rod. The bending stiffness of the rod can be described by the relation

$$B(x)=E(x)I(x), \tag{3.1}$$

where

$$E(x)=\bar{E}\left[1+\delta_E(x)\right],\ I(x)=\bar{I}(x)\left[1+\delta_I(x)\right], \tag{3.2}$$

which corresponds to the classical treatment of random variables in structural analysis (Melchers [23]; Ditlevsen *et al.* [24]), where $\bar{E}$ and $\bar{I}(x)$ denote the mean values, while $\delta_E(x)$ and $\delta_I(x)$ are random deviations with zero expected value

$$\mathbb{E}\delta_E(x)=\mathbb{E}\delta_I(x)=0 \tag{3.3}$$

and a specified variance:

$$Var\delta_E(x)=\sigma_E^2,\ Var\delta_I(x)=\sigma_I^2(x). \tag{3.4}$$

These deviations may additionally exhibit spatial correlation, reflecting the actual structure of the material

$$Cov\left[\delta_I(x_1),\delta_I(x_2)\right]=\sigma_I^2\exp\left(-|x_1-x_2|/\ell_c\right), \tag{3.5}$$

where l_c denotes the spatial correlation length. In the above expression, x_1 and x_2 denote two arbitrary coordinates along the rod for which the interdependence (covariance) of the deviations of the second moment of area $\delta_I(x)$ is defined. The parameter l_c characterizes the spatial range of dependence of geometric or

material fluctuations along the rod: for $|x_1 - x_2| \ll l_c$ the deviations $\delta_I(x_1)$ and $\delta_I(x_2)$ are strongly correlated, whereas for $|x_1 - x_2| \gg l_c$ they become effectively independent. Typically, the correlation length constitutes a fraction of the rod length, e.g. $l_c \approx (0.1–0.3)L$, corresponding to local manufacturing-related fluctuations. Such a correlation model allows for a realistic representation of spatially dependent imperfections along the rod. The correlation length l_c directly affects the covariance term entering the variance of the critical buckling load and may therefore influence the reliability-based assessment of the system response. The exponential covariance function provides a simple representation of short-range spatial correlation and ensures analytical tractability. Alternative correlation models, such as Gaussian or squared-exponential functions, would modify the covariance weighting and may therefore affect the variance of the critical buckling load; however, the proposed formulation is general with respect to the choice of the covariance kernel.

The introduction of the above relationships makes it possible to describe the bending stiffness of the rod as a random quantity (Elishakoff [25]):

$$B(x) = \overline{E}\,\overline{I}(x)\left[1 + \delta_E(x) + \delta_I(x) + \delta_E(x)\delta_I(x)\right]. \tag{3.6}$$

In the further considerations, it is assumed that the deviations are small ($|\delta_E|, |\delta_I| \ll 1$), which makes it possible to apply a linear approximation of the stochastic properties of the system. Under this assumption, higher-order terms in the perturbation expansion are neglected, and the resulting formulation is expected to be accurate for small to moderate levels of uncertainty. For larger uncertainty levels, higher-order effects may become non-negligible, potentially affecting both the mean value and the variance of the critical buckling load. Moreover, the global uncertainty δ_E describes the scatter of properties between specimens of the rod rather than along a single rod. This assumption reflects the fact that, for homogeneous structural materials, spatial variations of Young's modulus along an individual rod are typically much smaller than geometric deviations and can therefore be neglected. In this context, the uncertainty in E represents specimen-to-specimen variability rather than spatial fluctuations within a single element; for heterogeneous materials, a spatially varying description of $E(x)$ may be required.

To determine the influence of the randomness of the material and geometric parameters on the behavior of the rod in the buckled state, it is assumed that the differential equation of stability takes the form (Timoshenko and Gere [26])

$$\left(B(x)w''(x)\right)'' + F\,w''(x) = 0, \tag{3.7}$$

where $B(x)$ is the random bending stiffness defined according to relation (3.6), $w(x)$ denotes the transverse displacement of the rod axis (1), and F is the compressive force. The introduction of the random variables $\delta_E(x)$ and $\delta_I(x)$ causes the critical buckling load F_{kr} to also remain a random variable

$$F_{cr} = F_{cr}\left(E(x), I(x)\right). \tag{3.8}$$

In practice, however, a much more convenient form of analysis is the equivalent energetic form resulting from the Rayleigh – Ritz principle, in which the critical load is expressed by the so-called Rayleigh quotient, namely

$$\Rightarrow \int_0^L w(x)\left(B(x)w''(x)\right)''dx + F\int_0^L w(x)w''(x)dx = 0,$$

$$\Rightarrow \underbrace{\left[w(x)\left(B(x)w''(x)\right)'\right]_0^L}_{=0} - \int_0^L w'(x)\left(B(x)w''(x)\right)' dx + F\left(\underbrace{\left[w(x)w'(x)\right]_0^L}_{=0} - \int_0^L \left(w'(x)\right)^2 dx\right) = 0,$$

$$\Rightarrow -\int_0^L w'(x)\left(B(x)w''(x)\right)' dx - F\int_0^L \left(w'(x)\right)^2 dx = 0,$$

$$\Rightarrow -\underbrace{\left[w'(x)\left(B(x)w''(x)\right)\right]_0^L}_{=0} + \int_0^L B(x)\left(w''(x)\right)^2 dx - F\int_0^L \left(w'(x)\right)^2 dx = 0,$$

$$\Rightarrow \int_0^L B(x)\left(w''(x)\right)^2 dx - F\int_0^L \left(w'(x)\right)^2 dx = 0$$

$$\Rightarrow F_{cr} \approx \frac{\int_0^L B(x)\left(w''(x)\right)^2 dx}{\int_0^L \left(w'(x)\right)^2 dx}. \tag{3.9}$$

The form (3.9) is obtained from the stability equation after applying the principle in which the bending energy and the work of the compressive force are equal in the critical state.

Due to the fact that calculating the critical load in the stochastic formulation requires knowledge of its sensitivity to changes in the parameters, a perturbation expansion is introduced, making it possible to obtain a linear approximation of the influence of the uncertainties

3.1. Perturbation expansion

The result of the perturbation expansion is the derivation of analytical expressions for $\mathbb{E}F_{cr}$ and $VarF_{cr}$ as well as their sensitivities, which are needed in the definition of β and in the stationarity condition of the functional. For small deviations, i.e. for $|\delta_E|, |\delta_I| \ll 1$, a first-order Taylor expansion around the mean values can be applied, in accordance with the classical perturbation approach used in the stochastic analysis of structures (Liu *et al.* [27]; Kleiber *et al.* [28]):

$$F_{cr}(\delta_E, \delta_I) \approx F_{cr} + \frac{\partial F_{cr}}{\partial E}\delta_E + \int_0^L \frac{\delta F_{cr}}{\delta I(x)}\delta_I(x)dx, \tag{3.10}$$

where F_{kr} denotes the value of the critical load calculated for the mean parameter values $E = \bar{E}$, $I(x) = \bar{I}(x)$. From the expansion it follows that:

$$\mathbb{E}F_{cr} \approx F_{cr} \tag{3.11}$$

and

$$\mathrm{Var}F_{cr} = \sigma_E^2\left(\frac{\partial F_{cr}}{\partial E}\right)^2 + \sigma_I^2 \iint_\Omega \frac{\delta F_{cr}}{\delta I(x_1)}\frac{\delta F_{cr}}{\delta I(x_2)}\mathrm{Cov}\left[\delta_I(x_1), \delta_I(x_2)\right]dx_1 dx_2, \tag{3.12}$$

where $\Omega=[0,L]\times[0,L]$, while $\delta F_{kr}/\delta I(x_i)$ is the functional derivative, i.e., the quantity describing the sensitivity of the critical buckling load to a local change of the second moment of area at the point x_i. In other words, $\delta F_{kr}/\delta I(x_i)$ specifies how much the value of F_{kr}, will change if, in an infinitesimally small neighborhood of the point x_i the function $I(x)$ changes by an infinitesimal amount; formally

$$\delta F_{cr}=\int_0^L \frac{\delta F_{cr}}{\delta I(x)}\delta I(x)dx, \tag{3.13}$$

which corresponds to the linear sensitivity of the critical load F_{kr} to an infinitesimal perturbation of the function $I(x)$. Relations (3.11) – (3.13) make it possible to estimate the influence of geometric and material uncertainties on the expected value and variance of the critical buckling load, in accordance with the classical perturbation approach and the method of moments used in the stochastic analysis of structures (Liu *et al.* [27], Kleiber *et al.* [28]).

Due to the complexity of the mathematical framework, it is useful to compute the individual derivatives explicitly. As indicated earlier, Young's modulus E is spatially constant (a single rod is made of a homogeneous material – it is treated as a global random variable; this means that δ_E describes the scatter of properties between specimens of the rod, not fluctuations along a single element). Thus

$$\frac{\partial F_{cr}}{\partial E}=\frac{\partial}{\partial E}\left(\frac{E\int_0^L I(x)[w''(x)]^2\,dx}{\int_0^L [w'(x)]^2\,dx}\right)=\frac{\int_0^L I(x)[w''(x)]^2\,dx}{\int_0^L [w'(x)]^2\,dx}=\frac{1}{E}F_{cr}.$$

In turn, the functional derivative (if $F[y]=\int_a^b f(y(x),x)dx$ so $\frac{\delta F}{\delta y(x)}=\frac{\partial f}{\partial y}$; Gelfand *et al.* [29]).

$$\frac{\delta F_{cr}}{\delta I(x)}=\frac{\delta}{\delta I(x)}\left(\frac{E\int_0^L I(x)[w''(x)]^2\,dx}{\int_0^L [w'(x)]^2\,dx}\right)=\frac{E\,[w''(x)]^2}{\int_0^L [w'(x)]^2\,dx}.$$

3.2. Mean value and variance of the critical load – analytical development

On the basis of Eqs (3.11) and (3.12), the expression for the variance of the critical buckling load F_{kr} can be expressed explicitly in terms of the sensitivity functions and the spatial correlation function. For sufficiently small deviations $|\delta_E|,|\delta_I|\ll 1$ one obtains the relation:

$$\mathrm{Var}F_{cr}=\sigma_E^2\left(\frac{\partial F_{cr}}{\partial E}\right)^2+\sigma_I^2\iint_\Omega \frac{\delta F_{cr}}{\delta I(x_1)}\frac{\delta F_{cr}}{\delta I(x_2)}\exp\left(-|x_1-x_2|/\ell_c\right)dx_1dx_2, \tag{3.14}$$

where ℓ_c is the spatial correlation length, and the factor σ_I^2 arises from the definition of covariance (3.5). The sensitivity functions (of the critical load with respect to Young's modulus and the local second moment of area) are defined as follows

$$\Phi_E = \frac{\partial F_{cr}}{\partial E} = \frac{F_{cr}}{E_0}, \quad \Phi_I(x) = \frac{\delta F_{cr}}{\delta I(x)} = \frac{E\left(w''(x)\right)^2}{\int_0^L \left(w'(x)\right)^2 dx} = \frac{2\pi^2 E_0}{L^3}\sin^2\frac{\pi}{L}x. \tag{3.15}$$

Consequently, the variance can be written in a compact form:

$$VarF_{cr} = \sigma_E^2 \Phi_E^2 + \sigma_I^2 \iint_\Omega \Phi_I(x_1)\Phi_I(x_2)\exp\left(-|x_1 - x_2|/\ell_c\right)dx_1 dx_2. \tag{3.16}$$

Relations (3.14) – (3.16) make it possible to estimate the influence of geometric and material uncertainties on the expected value and variance of the critical buckling load, in accordance with the classical perturbation approach (Liu *et al.* [27], Kleiber *et al.* [28], Elishakoff [25]).

3.3. Reliability measure and limit-state function

In probabilistic analysis, the so-called *limit-state function* $g(\delta_E, \delta_I)$, is introduced, defined as the difference between the actual (random) critical load and the required design load F_p (corresponding to the design compressive load resulting from the load-bearing condition):

$$g(\delta_E, \delta_I) = F_{cr}(\delta_E, \delta_I) - F_p \tag{3.17}$$

and if the event $g > 0$ occurs, then the state is safe (load-bearing capacity greater than the required load), while when $g < 0$ a failure state occurs, in accordance with the classical formulation of structural reliability theory (Ditlevsen *et al.* [24]; Melchers [23]; Nowak *et al.* [30]). The reliability index can be written as (Hasofer *et al.* [31]):

$$\beta = \frac{\mathbb{E}[F_{cr}] - F_p}{\sqrt{\mathrm{Var}[F_{cr}]}}. \tag{3.18}$$

The required reliability level is defined by the condition:

$$\beta \geq \beta_p = 2.33, \tag{3.19}$$

which corresponds to the target safety probability $P(g > 0) \geq 0.99$ (Nowak *et al.* [30]). The target reliability index $\beta_p = 2.33$, corresponding to a probability of failure of approximately *1%*, is adopted as a representative moderate reliability level. Different choices of β_p would modify the reliability constraint, leading to more conservative solutions for higher reliability targets and less restrictive designs for lower values of β_p. Relations (3.17) – (3.19) make it possible to link the results of the variance analysis with the reliability assessment of the rod. Such a formulation enables a direct connection of the analytical model with probabilistic analysis and constitutes the basis for the shape optimization of the rod at a prescribed reliability level (Ditlevsen *et al.* [24], Melchers [23]). The obtained relations for the reliability index constitute the starting point for formulating the optimization problem with the constraint $\beta \geq \beta_p$.

3.4.Probabilistic shape optimization – "Gaussian profile"

The aim of the optimization is to determine the function $I(x)$, which minimizes the mass of the rod while maintaining the required reliability level β_p. The functional takes the form

$$J(I(x)) = \int_0^L \rho A(I(x))dx + \lambda\left[\beta_p - \beta(I(x))\right], \tag{3.20}$$

where λ is the Lagrange multiplier associated with the reliability constraint (Kleiber *et al.* [28]), while ρ denotes the material density and $A(I(x))$ the cross-sectional area corresponding to the second moment of area $I(x)$. The constraint $\beta_p - \beta(I(x)) = 0$ ensures that the required reliability level is satisfied. After including the perturbation expansion for $\beta(I(x))$, an analytical extremum condition is obtained, which leads to the solution:

$$I^*(x) = I_0 \exp a(x - L/2)^2\left[1 - k\sigma_I^2(x)\right], \tag{3.21}$$

where k is a correction coefficient dependent on the level of uncertainty (it specifies the intensity of the variance correction of the profile and is selected in such a way as to ensure satisfaction of the required reliability level β_p; its value depends on the relationship between the scatter of geometric parameters and the expected load capacity (Elishakoff [25], Kleiber *et al.* [28])).

Expression (3.21) defines the so-called Gaussian-type profile, in which the deterministic shape $I(x) = I_0 \exp a(x - L/2)^2$, has been corrected by a variance-related component associated with the local variance of the second moment of area. This profile makes it possible to limit the influence of geometric fluctuations on the reduction of the critical load while maintaining a minimal increase in the mass of the structure, or conversely. It therefore constitutes a compromise between lightness and reliability of the structure under uncertainty. Thus, solution (3.21) represents a probabilistic generalization of the deterministic Clausen–Gaussian profile, taking into account the influence of the variance of geometric parameters.

4. Numerical example

Having formulated the functional and the stationarity condition, we proceed to a numerical example, in which we first determine the deterministic profile and then the optimal profile satisfying β_p. For verification of the presented model, a numerical analysis was carried out on the example of a rod with variable bending stiffness, i.e. the following problem was solved: determine the optimal mass of a compressed rod, pinned at both ends, with a circular cross-section $(r = r(x))$, made of a material with Young's modulus E_0 and relative random deviations σ_E / E_0. The rod has length L, and its variable second moment of area is described by the relation $I(x) = I_0 \exp a(x - L/2)^2$, where I_0 denotes the value of the second moment of area at the mid-length of the rod, and a is the shape parameter of the profile. The geometric deviations are to be modeled as a random process with relative standard deviation σ_I / I_0 and spatial correlation length $\ell_c = 0,2L$. The buckling mode is assumed in the form $w(x) = A\sin \pi x / L$, where A denotes the buckling amplitude.

Data:

- ✓ rod length: $L = 1.5\,m,$
- ✓ second moment of area of the reference rod: $I_{ref} = 0.5 \cdot 10^{-7}\ m^4,$
- ✓ geometric deviations: $\sigma_I / I_0 = 0.09,$
- ✓ Young's modulus: $E_0 = 2.1 \cdot 10^5\ MPa,$
- ✓ relative random deviations of E_0: $\sigma_E / E_0 = 0.05,$
- ✓ density of the rod: $\rho = 7850\,kg / m^3,$
- ✓ reliability index: $\beta_p = 2.33,$
- ✓ required design load value: $F_p = 0.8 F_{kr,det}\,.$

Calculations for the reference rod

- ✓ critical load value:

$$F_{cr,ref} = \frac{\pi^2 E_0 I_{ref}}{L^2} = \frac{\pi^2 \cdot 2.1 \cdot 10^5\ MPa \cdot 0.5 \cdot 10^{-7}\ m^4}{(1.5\,m)^2} = 46.06\,kN,$$

- ✓ radius of the cross-section:

$$r_{ref} = \sqrt[4]{4 I_{ref} / \pi} = 0.0159\,m,$$

- ✓ mass:

$$m_{ref} = \rho V_{ref} = \rho \pi r_{ref}^2 L = 9.33\,kg.$$

Calculations for the deterministic rod

- ✓ Equation of equality of critical loads

In view of (3.9)

$$F_{cr,det}\left(a_{det}, I_{0,det}\right) \approx \frac{E_0 \int_0^L I_{det}(x)\left(w''(x)\right)^2 dx}{\int_0^L \left(w'(x)\right)^2 dx},$$

where $w = w(x)$ is defined by relation (1), and $I_{det}(x) = I_{0,det} \exp\left(a_{det}(x - L/2)^2\right).$ The equation of equality of critical loads reduces to the relation

$$F_{cr,det}\left(a_{det}, I_{0,det}\right) = F_{cr,ref}\,.$$

The above equation does not have a solution in analytical form; therefore, it was solved numerically using the Wolfram Mathematica environment (version 12.1). The calculations were carried out with the command FindRoot, with an adopted integration step $\Delta x = 0.001\ m$. This step size ensures stable numerical evaluation of the integrals involved, and the obtained results were found to be insensitive to moderate variations of the

discretization parameter. The process made it possible to identify the shape of the deterministic rod – its solution leads to

$$a_{det} = -1.675,\ I_{0,det} = 0.56 \cdot 10^{-7}\, m^4.$$

✓ mass

$$m_{det} = \rho V_{det} = \rho \int_0^L A_{det}(x)\,dx = \rho \int_0^L \sqrt{4\pi\, I_{det}(x)}\,dx = 8.52\,kg.$$

Comparison of the rod masses $\left(m_{det} / m_{ref}\right)$ shows that the deterministic rod is approximately 9 % lighter than the reference rod. Figure 4 presents a comparison of the radii of the cross-sections along the lengths of the analyzed rods.

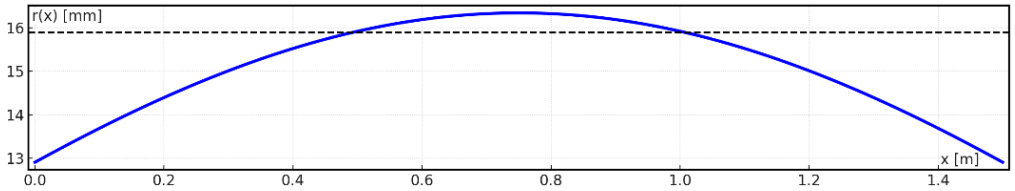

Fig.4. Comparison of the radii of the cross-sections of the rods (dashed line – reference rod, blue line – deterministic rod; scale not preserved).

✓ Expected value of the critical load (in view of (3.11)): $\mathbb{E}F_{cr} \approx 46.06\,kN$.

✓ Variance of the critical load; since

$$\Phi_{E,det} = \frac{F_{cr,det}}{E_0} \quad \text{and} \quad \Phi_I(x) = \frac{2\pi^2 E_0}{L^3} \sin^2 \frac{\pi}{L} x, \ \text{then}$$

$$Var F_{cr,\det} = \sigma_E^2 \Phi_{E,\det}^2 + \sigma_I^2 \iint_\Omega \Phi_I(x_1)\Phi_I(x_2) \exp\left(-|x_1 - x_2| / \ell_c\right) dx_1 dx_2 =$$

$$= \left(0.05 E_0\right)^2 \left(\frac{F_{cr,det}}{E_0}\right)^2 + \left(0.09 I_{0,det}\right)^2 \left(\frac{2\pi^2 E_0}{L^3}\right)^2 \times$$

$$\times \iint_\Omega \Phi_I(x_1)\Phi_I(x_2) \exp\left(-|x_1 - x_2| / \ell_c\right) dx_1 dx_2 = 25 \cdot 10^{-4} \left(46.06 kN\right)^2 +$$

$$+ \left(0.09 \cdot 0.56 \cdot 10^{-7}\, m^4\right)^2 \left(\frac{2\pi^2 \cdot 2.1 \cdot 10^5\, MPa}{\left(1.5\, m\right)^3}\right)^2 \cdot 0.252\, m^2 = 1.496 \cdot 10^7\, N^2.$$

✓ Reliability index:

$$\beta = \frac{\mathbb{E}F_{cr,det} - F_p}{\sqrt{\mathrm{Var} F_{cr,det}}} = \frac{F_{cr,det} - 0.8 F_{cr,det}}{\sqrt{\mathrm{Var} F_{cr,det}}} = \frac{0.2 \cdot 46.06 \cdot 10^3\, N}{\sqrt{1.496 \cdot 10^7\, N^2}} = 2.38,$$

– which shows that condition (3.19) remains satisfied.

After determining the parameters of the deterministic rod, the next step is to determine the shape of the rod that is optimal in the probabilistic sense.

Calculations for the optimal profile

✓ Variation of the functional (3.20)

$$\delta J = \int_0^L \rho \frac{dA\left(I(x)\right)}{dI} \delta I(x) dx - \lambda \delta\beta. \tag{4.1}$$

In view of the fact that

$$\beta = \frac{F_{cr,opt} - F_p}{\sqrt{\mathrm{Var} F_{cr,opt}}},$$

the variation is

$$\delta\beta = \frac{\delta\left(F_{cr,opt} - F_p\right)\sqrt{VarF_{cr,opt}} - \left(F_{cr,opt} - F_p\right)\delta\sqrt{VarF_{cr,opt}}}{VarF_{cr,opt}} =$$

$$= \frac{\delta F_{cr,opt}\ \sqrt{VarF_{cr,opt}} - \left(F_{cr,opt} - F_p\right)\dfrac{\delta VarF_{cr,opt}}{2\sqrt{VarF_{cr,opt}}}}{VarF_{cr,opt}} =$$

$$= \frac{\delta F_{cr,opt}}{\sqrt{VarF_{cr,opt}}} - \frac{F_{cr,opt} - F_p}{2\left(\sqrt{VarF_{cr,opt}}\right)^3} \delta VarF_{cr,opt}.$$

Furthermore, the variance of the critical load

$$VarF_{cr,opt} = \sigma_E^2 \Phi_E^2 + \sigma_I^2 \iint_\Omega \Phi_I\left(x_1\right)\Phi_I\left(x_2\right)\exp\left(-|\,x_1 - x_2|\,/\ell_c\right)dx_1 dx_2 =$$

$$= \left(0.05E_0\right)^2\left(\frac{F_{cr,opt}}{E_0}\right)^2 + \left(0.09I_{0,opt}\right)^2\left(\frac{2\pi^2 E_0}{L^3}\right)^2 \times$$

$$\times \iint_\Omega \sin^2\frac{\pi}{L}x_1 \sin^2\frac{\pi}{L}x_2 \exp\left(-|\,x_1 - x_2|\,/\ell_c\right)dx_1 dx_2 =$$

$$= 25\cdot 10^{-4}\left(F_{cr,opt}\right)^2 + \left(0.09\cdot I_{0,opt}\right)^2\left(\frac{2\pi^2\cdot 2.1\cdot 10^5\ MPa}{\left(1.5\,m\right)^3}\right)^2 \cdot 0.252\,m^2,$$

that is

$$VarF_{cr,opt} = 25\cdot 10^{-4}\left(F_{cr,opt}\right)^2 + 3.079\cdot 10^{21}\left(I_{0,opt}\right)^2, \tag{4.2}$$

whence

$$\delta VarF_{cr,opt} = 50 \cdot 10^{-4} F_{cr,opt}\, \delta F_{cr,opt} + 6.158 \cdot 10^{21} I_{0,opt}\, \delta I_{0,opt}. \tag{4.3}$$

However, from relation (3.13) and the second relation (3.15)

$$\delta F_{cr,opt} = \int_0^L \Phi_I(x) \delta I(x) dx \tag{4.4}$$

and taking this into account

$$\delta VarF_{cr,opt} = 50 \cdot 10^{-4} F_{cr,opt} \int_0^L \Phi_I(x) \delta I(x) dx + 6.158 \cdot 10^{21} I_{0,opt}\, \delta I_{0,opt} \tag{4.5}$$

and finally, the variation

$$\begin{aligned} \delta\beta = &\left(\frac{1}{\sqrt{VarF_{cr,opt}}} - 25 \cdot 10^{-4} \frac{F_{cr,opt} - F_p}{\left(\sqrt{VarF_{cr,opt}}\right)^3} F_{cr,opt} \right) \int_0^L \Phi_I(x) \delta I(x) dx + \\ &- \frac{F_{cr,opt} - F_p}{2\left(\sqrt{VarF_{cr,opt}}\right)^3} 6.158 \cdot 10^{21} I_{0,opt}\, \delta I_{0,opt}. \end{aligned} \tag{4.6}$$

In view of the above, the variation (4.1) takes the form

$$\begin{aligned} \delta J = &\int_0^L \rho \frac{dA(I(x))}{dI} \delta I(x) dx - \lambda \left(\frac{1}{\sqrt{VarF_{cr,opt}}} - 25 \cdot 10^{-4} \frac{F_{cr,opt} - F_p}{\left(\sqrt{VarF_{cr,opt}}\right)^3} F_{cr,opt} \right) \times \\ &\times \int_0^L \Phi_I(x) \delta I(x) dx + \lambda \frac{F_{cr,opt} - F_p}{2\left(\sqrt{VarF_{cr,opt}}\right)^3} 6.158 \cdot 10^{21} I_{0,opt}\, \delta I_{0,opt}, \end{aligned} \tag{4.7}$$

- ✓ the stationarity equation $\delta J = 0$ takes the form

$$\begin{aligned} &\int_0^L \rho \frac{dA(I(x))}{dI} \delta I(x) dx - \lambda \left(\frac{1}{\sqrt{VarF_{cr,opt}}} - 25 \cdot 10^{-4} \frac{F_{cr,opt} - F_p}{\left(\sqrt{VarF_{cr,opt}}\right)^3} F_{cr,opt} \right) \times \\ &\times \int_0^L \Phi_I(x) \delta I(x) dx + \lambda \frac{F_{cr,opt} - F_p}{2\left(\sqrt{VarF_{cr,opt}}\right)^3} 6.158 \cdot 10^{21} I_{0,opt}\, \delta I_{0,opt} = 0. \end{aligned} \tag{4.8}$$

The last equation constitutes the necessary optimality condition in the variational sense. To enable its practical solution, a family of functions describing the distribution of the second moment of area is adopted in the form

$I(x) = I_{0,opt} \exp(a_{opt}\left(x - L/2\right)^2)$, where $I_{0,opt}$ denotes the value of the second moment of area at the mid-length of the rod, and a_{opt} is the shape parameter of the profile. This assumption reduces the problem to two decision variables $\left(I_{0,opt}, a_{opt}\right)$, which makes it possible to pass from the continuous formulation to a parametric one. In this formulation, the functional J takes the form:

$$J\left(I_{0,opt}, a\right) = m\left(I_{0,opt}, a_{opt}\right) + \lambda\left[\beta_p - \beta\left(I_{0,opt}, a_{opt}\right)\right], \tag{4.9}$$

where m denotes the mass of the rod, and β is the reliability index dependent on the adopted critical load and its variance. The stationarity condition $\delta J = 0$ leads to a system of three nonlinear equations:

$$\partial_{I_{0,opt}} J = 0,\ \partial_{a_{opt}} J = 0,\ \beta_p - \beta\left(I_{0,opt}, a_{opt}\right) = 0, \tag{4.10}$$

which constitute the basis for further numerical analysis. The computational algorithm obtained in this way is therefore the counterpart of the stationarity Eq.(4.8) – both express the same optimality condition, but in different spaces: variational and discrete. However, the system of stationarity Eqs (4.10) does not have a solution in analytical form. For this reason, the system was solved numerically using the Wolfram Mathematica environment. As before, the *FindRoot* command was used, which made it possible to determine simultaneously the pair of parameters $a_{opt}, I_{0,opt}$ and the Lagrange multiplier λ, which are as follows:

$$a_{opt} = -2.26, \qquad I_{0,opt} = 0.58 \cdot 10^{-7}\ m^4,\ \lambda = -3.07, \tag{4.11}$$

with the deterministic solution $\left(I_{0,det}, a_{det}\right)$ adopted as the initial values. At each step of the numerical iteration, the integration step $\Delta x = 0.001\ m$ was used. This made it possible to maintain consistency with the earlier part of the analysis (deterministic profile), and at the same time to take into account the influence of the random parameters σ_E / E_0 and $\sigma_I / I_{0,opt}$ on the value of the reliability index β. The applied procedure made it possible to identify the shape of the rod that is optimal in the probabilistic sense, i.e. with minimal mass while maintaining the required reliability level β_p. Mass of the optimal rod

$$m_{opt} = \rho V_{opt} = \rho \int_0^L A_{opt}(x)\,dx = \rho \int_0^L \sqrt{4\pi\, I_{opt}(x)}\,dx = 8.27\,kg.$$

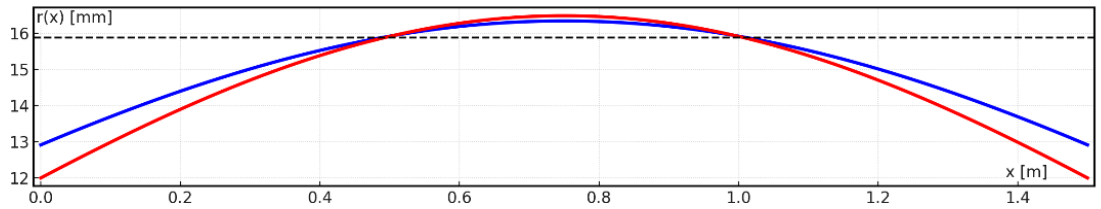

Fig.5. Comparison of the radii of the cross-sections of the rods (dashed line – reference rod, blue line – deterministic rod, red line – optimal rod; scale not preserved).

The comparison of the masses of the rods $\left(m_{opt} / m_{det}\right)$ shows that the optimal rod is about *3%* lighter than the deterministic rod and about *12%* lighter than the reference rod $\left(m_{opt} / m_{ref}\right)$. Figure 5 presents a comparison of the radii of the cross-sections of all rods.

5. Conclusions and summary

The conducted analysis demonstrates that incorporating material and geometric uncertainties into the design process of compressed rods enables the development of structural solutions that are not only lighter, but also more predictable in terms of buckling load capacity. In contrast to purely deterministic formulations, the proposed stochastic approach allows for a quantitative assessment of the influence of local fluctuations in bending stiffness on the critical buckling load, thereby providing a more realistic and reliability-oriented evaluation of structural safety.

By employing a first-order perturbation expansion, analytical expressions for the expected value and variance of the critical buckling load were derived, together with sensitivity measures describing the influence of random material and geometric parameters. The incorporation of these relations into the objective function made it possible to formulate a probabilistic shape optimization problem subject to a prescribed reliability constraint. The resulting solution, expressed in the form of a Gaussian-type stiffness profile, can be interpreted as a probabilistic generalization of the classical Gauss profile, explicitly reflecting the local sensitivity of the structure to perturbations of the second moment of area.

The numerical results confirm the effectiveness of the proposed framework. The optimized deterministic profile yields a mass reduction of approximately *9%* relative to the reference rod, while the probabilistic optimization leads to an additional reduction of about *3%* without violating the required reliability level. These results indicate that explicit modeling of material and geometric variability creates additional opportunities for material savings and can significantly enhance the efficiency of lightweight structural members while maintaining an adequate safety margin.

The reported mass reduction should be interpreted in the context of the adopted analytical – stochastic framework. Although larger mass reductions or higher increases in load-carrying capacity have been reported in the literature using advanced deterministic or purely numerical optimization techniques, the objective of the present study is not to outperform such approaches in terms of absolute efficiency. Instead, the contribution of this work lies in identifying additional regions of material savings that emerge when uncertainty and reliability requirements are explicitly integrated into the optimization process, thereby complementing existing shape optimization strategies.

The present study focuses on a transparent analytical formulation that allows the influence of uncertainty on the critical buckling load to be isolated and interpreted in a physically meaningful way. Within this framework, the results provide a consistent basis for further investigations and methodological extensions, including alternative admissible shape functions and broader classes of reliability constraints.

The developed analytical–stochastic framework is deliberately limited to linear Euler buckling of a pinned–pinned rod and to a first-order perturbation-based reliability formulation. Extensions to other boundary conditions, geometric nonlinearities, initial imperfections, post-buckling behavior, experimental or numerical validation, as well as applications to thin-walled or truss structures, would require fundamentally different kinematic and energetic formulations and are therefore left for future research.

Nomenclature

a – profile shape coefficient,
$B(x)$ – bending stiffness of the rod,
Cov – covariance,
E – Young's modulus,
$\mathbb{E}$ – expected value,

F_{cr} – critical load,

F_p – design load,

g – limit-state function,

$I(x)$ – variable cross-sectional moment of inertia of the rod,

I_0 – moment of inertia at the mid-length of the rod,

J – functional,

ℓ_c – spatial correlation length,

Var – variance,

$w(x)$ – buckling mode shape,

β – reliability index,

δ – first variation of the functional,

$\delta_E(x)$ – random deviation of Young's modulus,

$\delta_I(x)$ – random deviation of the cross-sectional moment of inertia,

λ – Lagrange multiplier,

$\cdots_{det}$ – footnote relating to the deterministic rod,

$\cdots_{opt}$ – footnote relating to the optimal rod,

$\cdots_{ref}$ – footnote relating to the reference rod.

References

[1] Lagrange J.L. (1773): *Essai d'une nouvelle méthode pour déterminer les maxima et les minima des formules intégrales indéfinies*.– Miscellanea Taurinensia, vol.6, pp.173-195.

[2] Clausen T. (1851): *Über die Form des kräftigsten Pfeilers von gleicher Länge und Masse*.– Journal für die reine und angewandte Mathematik, vol.41, pp.321-328.

[3] Blasius H. (1910): *Über die Form des stabilsten Stabes*.– Zeitschrift für Math. und Physik, vol.58, pp.1-20.

[4] Ratzerdorfer O. (1921): *Über die Festigkeit von Säulen mit veränderlichem Querschnitt*.– Zeitschrift für Angewandte Mathematik und Mechanik, vol.1, pp.151-164.

[5] Jasiński F.S. (1894): *De la flexion des colonnes avec imperfections initiales*.– Annales des Ponts et Chaussées, vol.8, No.4, pp.312-336.

[6] Keller J.B. and Tadjbakhsh I. (1962): *Strongest column and isoperimetric inequalities for eigenvalues*.– Journal of Mathematical Physics, vol.5, No.4, pp.646-650.

[7] Gajewski A. (1966): *On the optimal shaping of slender rods made of a nonlinearly elastic material*.– Theoretical and Applied Mechanics, vol.4, No.4, pp.637-656.

[8] Gajewski A. (1975): *Shape Optimization of Thin-Walled Rods*.– WNT, Warszawa.

[9] Filipow A.P. and Griniew W.B. (1975-1979): *Optimalnye Konstrukcii Elementov Nesuschich System*.– Strojizdat, Moskva.

[10] Atanacković T.M. and Simić S.S. (1999): *On the optimal shape of a Pflüger column*.– Eur. J. Mech. A/Solids, vol.18, No.5, pp.903-913, https://doi.org/10.1016/S0997-7538(99)00128-X.

[11] Erdönmez Ü. and Özkol I. (2010): *Optimal shape analysis of a column structure under various loading conditions by using differential transform method (DTM)*.– Applied Mathematics and Computation, vol.216, pp.3172-3183, https://doi.org/10.1016/j.amc.2010.04.036.

[12] Parastesh H., Hajirasouliha I., Taji H. and Bagheri Sabbagh A. (2019): *Shape optimization of cold-formed steel beam-columns with practical and manufacturing constraints*.– Journal of Constructional Steel Research, vol.155, pp.249-259, https://doi.org/10.1016/j.jcsr.2018.12.031.

[13] Marcinowski J. and Sadowski M. (2020): *Using the ERFI function in the problem of the shape optimization of the compressed rod*.– International Journal of Applied Mechanics and Engineering, vol.25, No.2, pp.75-87, https://doi.org/10.2478/ijame-2020-0021.

[14] Marcinowski J. and Sadowski M. (2021): *Designing of steel CHS columns showing maximum compression resistance*.– Civil and Environmental Engineering Reports, vol.31, No.1, pp.79-92, https://doi.org/10.2478/ceer-2021-0006.

[15] Botis M.F. and Cerbu C. (2022): *Design solutions for slender bars with variable cross-sections to increase the critical buckling force*.– Materials, vol.15, No.17, p.6094, https://doi.org/10.3390/ma15176094.

[16] Xu T., Huang X., Lin X. and Xie Y.M. (2023): *Topology optimization for maximizing buckling strength using a linear material model*.– Computer Methods in Applied Mechanics and Engineering, vol.417, p.116437, https://doi.org/10.1016/j.cma.2023.116437.

[17] Uysal M.U. (2023): *Effects of cryogenically treated CFRP composite on the buckling behavior in the adhesively bonded beam*.– Journal of Engineering Sciences, vol.10, No.1, pp.D1-D7, https://doi.org/10.21272/jes.2023.10(1).d1.

[18] Dahlberg V., Dalklint A., Spicer M., Amir O. and Wallin M. (2023): *Efficient buckling constrained topology optimization using reduced order modeling*.– Structural and Multidisciplinary Optimization, vol.66, p.161, https://doi.org/10.1007/s00158-023-03616-7.

[19] Ruocco E., Forooghi A. and Pellecchia D. (2024): *Shape Optimization of Hencky-Type Reddy Columns Against Buckling Using Genetic Algorithms and Artificial Neural Networks*.– SSRN Preprint, https://doi.org/10.2139/ssrn.5352695.

[20] Ferrari F. and Sigmund O. (2025): *Optimization of the initial post-buckling response of trusses and frames by an asymptotic approach*.– Int. Journal for Numerical Methods in Engineering, https://doi.org/10.1002/nme.70082.

[21] Morse L., Cartabia L. and Mallardo V. (2022): *Reliability-based bottom-up manufacturing cost optimisation for composite aircraft structures*.– Structural and Multidisciplinary Optimization, vol.65, p.159, https://doi.org/10.1007/s00158-022-03250-9.

[22] Ferreira Filho J.O., Simões da Silva L., Tankova T. and Carvalho H. (2024): *Influence of geometrical imperfections and residual stresses on the reliability of high strength steel welded I-section columns using Monte Carlo simulation*.– J. of Constructional Steel Research, vol.215, p.108548, https://doi.org/10.1016/j.jcsr.2024.108548.

[23] Melchers R.E. (1999): *Structural Reliability: Analysis and Prediction*.– John Wiley & Sons, Chichester.

[24] Ditlevsen O. and Madsen H.O. (1996): *Structural Reliability Methods*.– John Wiley & Sons, Chichester.

[25] Elishakoff I. (1999): *Probabilistic Theory of Structures*.– Dover Publications, New York.

[26] Timoshenko S.P. and Gere J.M. (1961): *Theory of Elastic Stability*.– McGraw-Hill Book Comp., New York.

[27] Liu W.K. and Der Kiureghian A. (1986): *Finite element reliability methods for stochastic structures*.– Journal of Engineering Mechanics, vol.112, No.1, pp.85-104.

[28] Kleiber M. and Hien T.D. (1992): *The Stochastic Finite Element Method: Basic Perturbation Technique and Computer Implementation*.– John Wiley & Sons, New York.

[29] Gelfand I.M. and Fomin S.V. (1963): *Calculus of Variations*.– Prentice-Hall, Englewood Cliffs, New York.

[30] Nowak A.S. and Collins K.R. (2013): *Reliability of Structures*.– CRC Press, Boca Raton.

[31] Hasofer A.M. and Lind N.C. (1974): *Exact and invariant second-moment code format*.– Journal of the Engineering Mechanics Division, vol.100, No.1, pp.111-121, https://doi.org/10.1061/JMCEA3.0001848.

Received: December18, 2025
Revised: March 26, 2026